

# Electrostatic Modulation of Aromatic Rings via Explicit Solvation of Substituents

Kamila B. Muchowska, Catherine Adam, Ioulia K. Mati, and Scott L. Cockroft\*

EaStCHEM School of Chemistry, University of Edinburgh, King's Buildings, West Mains Road, Edinburgh EH9 3JJ, U.K.

**S** Supporting Information

**ABSTRACT:** Solvent effects are implicated as playing a major role in modulating electrostatic interactions via through-space and polarization effects, but these phenomena are often hard to dissect. By using synthetic molecular torsion balances and a simple explicit solvation model, we demonstrate that the solvation of substituents substantially affects the electrostatic potential of aromatic rings. Although polarization effects are important, we show that a simple additive through-space model also provides a reasonable account of the experimental data. The results deliver insights into solvent structure and might contribute to the development of computationally inexpensive solvent models.

Molecular recognition is determined by many factors, among which the electrostatic components have been identified as being one of the most important.<sup>1–3</sup> However, unraveling the complicated influence of solvents on the behavior of chemical and biological systems remains a long-standing challenge.<sup>3–5</sup> Indeed, solvation is implicated in governing the rate and outcome of chemical reactions,<sup>5–7</sup> the structure of biological molecules,<sup>8</sup> and the position of supramolecular and conformational equilibria.<sup>9–19</sup> For instance, the specific solvation of substituents has been attributed to  $pK_a$  changes in positions several atoms away.<sup>20–22</sup> However, combined experimental and theoretical approaches capable of unambiguously identifying the specific electronic effects of substituent solvation are required.

Here we have synthesized a series of simple molecular torsion balances for measuring the electronic properties of aromatic rings as the solvent and substituents are varied (Figure 1). Comparison of experimental conformational energies with calculated electrostatic potentials (Figure 2) has enabled quantification of the modulating effects arising from substituent solvation (Figure 3), and an examination of the predictive capacity of (force-field-like) through-space models of long-range electrostatic effects (Figure 4).

The concept of using conformationally interchangeable molecular probes for measuring weak interactions was introduced by Ōki,<sup>23</sup> and later popularized by Wilcox,<sup>24,25</sup> who coined the phrase “molecular torsion balances” to describe these types of systems. Since then, molecular torsion balances have been used to investigate a diverse range of non-covalent interactions.<sup>9–15,26–33</sup> The molecular torsion balances employed in this study exist in equilibrium between two conformational states (Figure 1). Due to the partial double-

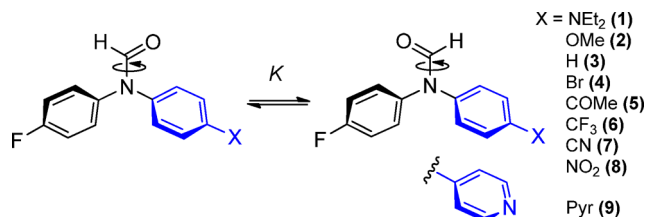


**Figure 1.** Molecular torsion balances used in this study. Rotation about the formamide group is slow on the NMR time scale, thus allowing electronic and solvent effects on the conformational free energy  $\Delta G_{\text{exp}}$  to be determined via integration of the  $^{19}\text{F}$  NMR peaks corresponding to each conformer.

bond character of the formamide C–N bond, the rate of interconversion between the formyl rotamers is slow on the NMR time scale. Thus, integration of  $^{19}\text{F}$  NMR peaks corresponding to each conformer allows accurate determination of the equilibrium constant,  $K$ , and the conformational free energy,  $\Delta G_{\text{exp}} = -RT \ln K$ .

In accord with the behavior of other molecular torsion balances, the position of the conformational equilibrium is sensitive to the electronic effects of substituents.<sup>9–13</sup> As shown in Table 1, we found that  $\Delta G_{\text{exp}}$  values measured in apolar organic solvents correlated well with  $\sigma_m$  Hammett substituent constants ( $R^2 = 0.95–0.98$ , Figure S6), but less well with  $\sigma_p$  ( $R^2 = 0.85–0.95$ , Figure S7).<sup>34</sup> The correlation with  $\sigma_m$  can be attributed to intramolecular interactions occurring between the formyl group and the *meta* positions on each side of the balance (which come into close proximity due to the propeller-like twist of the aromatic rings). Thus, the formyl oxygen prefers to reside over the least electron-rich X-substituted ring when  $X = \text{NO}_2$ , while the other conformer is preferred when  $X = \text{NEt}_2$  (Figure 1).

Consistent with this hypothesis,  $\Delta G_{\text{exp}}$  values obtained in benzene- $d_6$  also gave excellent correlations (open circles in Figure 2a) with gas-phase calculated electrostatic potentials taken directly over the carbon atoms *meta* to the X-substituent of simple mono-substituted benzenes ( $\text{ESP}_{\text{gas}}$ , left column in Figure 3, Table 1). In contrast,  $\Delta G_{\text{exp}}$  values measured in chloroform- $d$  showed significant scatter when plotted against the same  $\text{ESP}_{\text{gas}}$  values (open circles in Figure 2b). Similar, but less noticeable scattering was also seen in dichloromethane and carbon tetrachloride (Figure S11). Such scattering cannot be easily attributed to the dielectric effects of the solvent, nor the

Received: March 12, 2013

**Table 1. Correlation Coefficients ( $R^2$ ) of  $\Delta G_{\text{exp}}$  Plotted against Hammett Substituent Constants and Electrostatic Potentials<sup>a</sup>**

property plotted	$R^2$ of plots against $\Delta G_{\text{exp}}$			
	$\text{CCl}_4$	benzene	DCM	chloroform
Hammett Constants				
$\sigma_p$	0.866	0.949	0.877	0.853
$\sigma_m$	0.947	0.971	0.977	0.974
Electrostatic Potentials				
$\text{ESP}_{\text{gas}}$	0.985	0.976	0.968	0.958
$\text{ESP}_{\text{SM8}}$	0.978	0.969	0.944	0.941
$\text{ESP}_{\text{solvx1}}$	0.995	0.987	0.992	0.994
$\text{ESP}_{\text{gas}} + \text{ESP}_{\text{through-space}}$	n.d. <sup>b</sup>	0.975	0.990	0.990

<sup>a</sup>Electrostatic potentials taken over positions *meta* to the substituent:  $\text{ESP}_{\text{gas}}$ , determined in the gas phase;  $\text{ESP}_{\text{SM8}}$ , determined using the implicit SM8 solvation model;  $\text{ESP}_{\text{solvx1}}$ , determined including a single explicit solvent molecule; and  $\text{ESP}_{\text{gas}} + \text{ESP}_{\text{through-space}}$ , determined including a single explicit solvent molecule where polarization effects were neglected. The corresponding graphs are shown in Figures 2, S6, S7, and S11–S13. <sup>b</sup>The through-space ESP was not determined for  $\text{CCl}_4$  due to the low polarity of this solvent.

solvation of the common features of each balance (such as the formyl groups or aromatic rings), which would be expected to influence the gradients of the plots in each solvent. Furthermore, the use of calculated ESPs in which the implicit SM8 solvation model was applied did not correct the scatter ( $\text{ESP}_{\text{SM8}}$ ; Table 1, Figure S12). Closer examination of the scattering in Figure 2b (chloroform) showed that the X = H point was shifted to the left relative to the X = OMe and  $\text{NEt}_2$  points. Interestingly, “outlying behavior” of H-substituted rings has previously been reported in  $\text{pK}_a$  studies where the solvation of substituents was implicated as playing a role.<sup>21</sup> Thus, since chloroform is a reasonably good hydrogen-bond donor, and the OMe and  $\text{NEt}_2$  substituents are hydrogen bond acceptors (while H clearly is not), we reasoned that the scatter in our correlations might result from differences in the solvation of the variable X-substituents.

To test the hypothesis that substituent solvation might be significantly affecting the electrostatic potentials of the aromatic rings in our molecular balances, we performed the usual B3LYP/6-31G\* ESP calculations, but the geometry optimizations were started with a single solvent molecule positioned near to the X-substituent. Solvent molecules were found to localize over the sites of the ESP minima seen in the unsolvated aromatics, which were located over the X-substituents in all cases (Figure 3). Furthermore, the electrostatic modulation of the adjacent aromatic rings was seen to be dependent on the solvent and identity of each substituent (Figure 3). Strikingly, we found that plotting our experimental  $\Delta G_{\text{exp}}$  values against the new ESPs (in which substituent solvation was explicitly modeled) decreased the scatter of the correlations for chloroform, dichloromethane, benzene, and carbon tetrachloride ( $\text{ESP}_{\text{solvx1}}$  in Table 1, filled points in Figures 2 and S11).

Indeed, the correlations improved to such an extent that the X = H points were no longer outliers relative to the X = OMe and  $\text{NEt}_2$  points. To further test this model we synthesized balance **9**, which features a pyridyl nitrogen in place of the X-substituent (Figure 1). We reasoned that solvation of a strong hydrogen-bond acceptor that is directly bonded to the aromatic ring would give rise to even larger ESP deviations than those seen for other substituents. Gratifyingly, even though the ESP

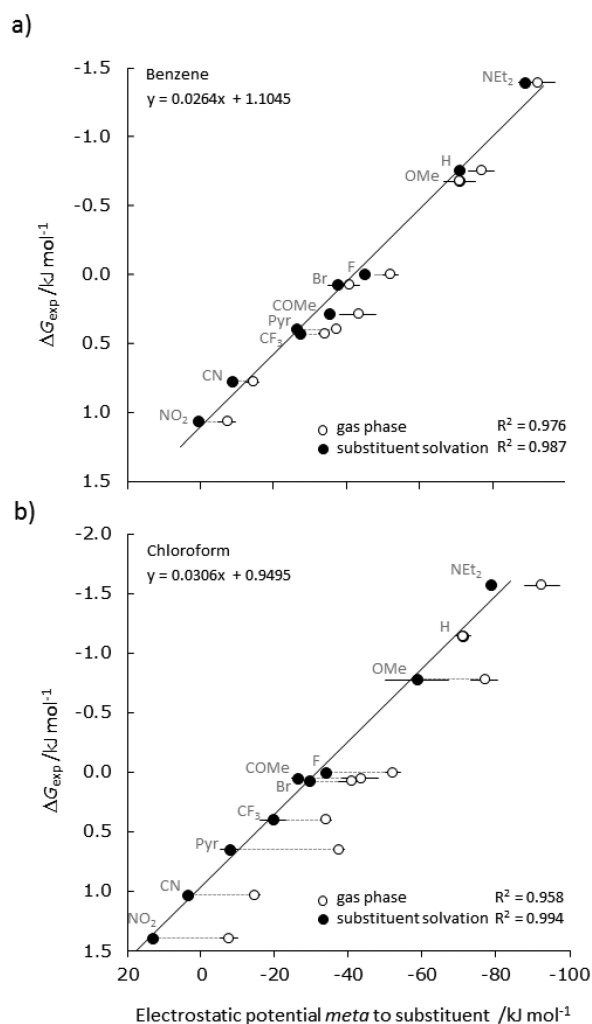


**Figure 2.** Experimental conformational free energies  $\Delta G_{\text{exp}}$  measured in (a) benzene- $d_6$  and (b) chloroform- $d$  at 298 K plotted against B3LYP/6-31G\* electrostatic surface potentials taken *meta* to the substituent, ESP. The open circles correspond to gas-phase calculations ( $\text{ESP}_{\text{gas}}$ , left column in Figure 3), while the filled circles correspond to calculations where the substituent is solvated by a single explicit solvent molecule ( $\text{ESP}_{\text{solvx1}}$ , center and right columns in Figure 3). The dotted lines correspond to  $\Delta \text{ESP}_{\text{meta}}$  for each substituent (as used in Figure 4). Horizontal error bars correspond to standard deviation in the electrostatic potential readings taken over both *meta* positions on each side of the aromatic ring (see SI). The plots for dichloromethane and carbon tetrachloride are provided in the SI. Errors in  $\Delta G_{\text{exp}}$ , estimated to be  $\pm 0.12$  kJ/mol (see SI), are omitted for the sake of clarity. All data are provided in Tables S1 and S2. Data for X = F corresponds to the hypothetical molecule where  $\Delta G_{\text{exp}} = 0$  by virtue of its symmetry.

over the *meta* position changes by +30 kJ/mol upon solvation with chloroform (Pyr in Figures 2 and 3), these data fit on the trend lines in all of the solvents examined (filled circles), while the unsolvated ESP data points (open circles) are the largest outliers in the plots shown in Figures 2 and S11. Although the improvements in the correlation coefficients upon considering substituent solvation appear relatively modest (Table 1), the absolute changes in the ESPs are quite substantial; a 30 kJ/mol ESP change is equivalent to replacing an OMe substituent with a halogen substituent in the gas phase (Table S1, Figure S3).

Figure 3 highlights another important effect of substituent solvation. It can be seen that ESPs taken over the rings when X

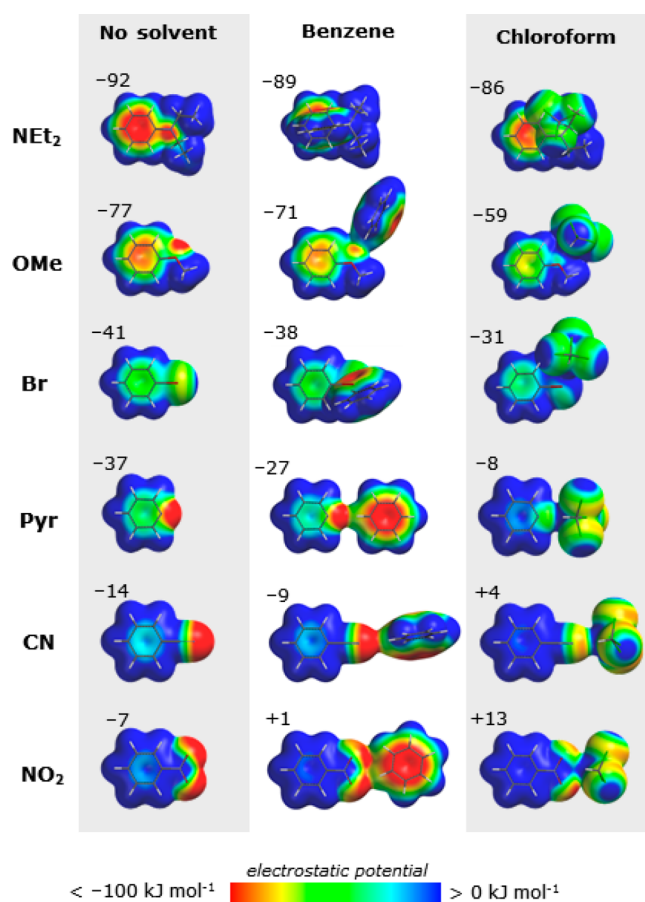


**Figure 3.** Effects of substituent solvation on electrostatic potential surfaces (ESPs) for a range of aromatic molecules calculated using B3LYP/6-31G\*. Numbers indicate the ESP taken over the *meta* position,  $ESP_{\text{gas}}$ , or  $ESP_{\text{solv}\times 1}$ . A version of this figure showing all solvents and substituents investigated is provided in the SI.

= NO<sub>2</sub> and X = CN change sign upon solvation, but still fit on the graphs shown in Figures 2 and S11. Consistent with this ESP sign inversion, numerous experimental trends involving aromatic interactions have been seen to reverse upon the introduction of nitro substituents in chloroform solution, including influences on conformational equilibria,<sup>35</sup> the stabilization of transition states,<sup>36</sup> edge-to-face,<sup>37,38</sup> stacking,<sup>39,40</sup> and cation- $\pi$  interactions.<sup>15</sup>

Overall, the range of substituents examined and the quality of the correlations shown in Figures 2 and S11, provides compelling evidence of notable electrostatic modulation of aromatic rings due to explicit solvation of substituents. Both through-space and polarization effects<sup>13,30,41-44</sup> have been proposed to contribute to long-range electrostatic effects, but it has also been shown that additive through-space models often serve as a reasonable approximation in some situations. Thus, we set about examining the utility of a simplified through-space approach for modeling the long-range electrostatic effects of substituent solvation.

Of the solvents examined, chloroform exerts the largest electrostatic changes when it solvates a particular substituent (Figure 3), and therefore provides the best opportunity for examining the utility of a through-space model. Figure 4 shows the electrostatic field originating from a single chloroform molecule in two examples of the minimized geometries shown in Figure 3. In accord with previous findings,<sup>44</sup> the bar graphs in

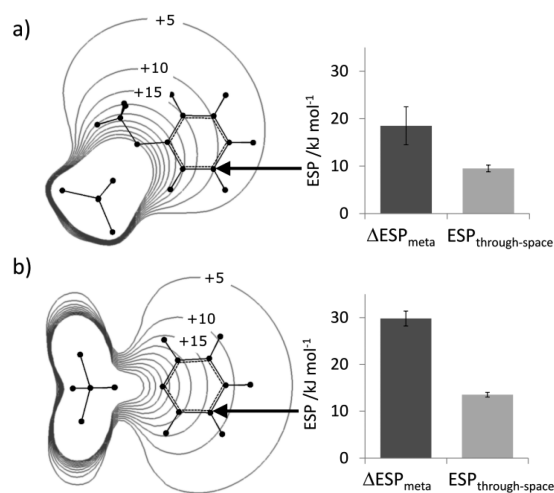


**Figure 4.** Through-space electrostatic potentials emanating from the partial positive charge of the polar C-H bond in chloroform for (a) an OMe-substituted phenyl ring and (b) a pyridyl ring. The electrostatic potential field ( $ESP_{\text{through-space}}$ ) was calculated for chloroform in isolation (using B3LYP/6-31G\*) and overlaid on the minimized structures shown in Figure 3. The electrostatic potential slices lie parallel to the plane of the aromatic ring and intersect the indicated *meta* positions on the 0.002 electron/Bohr<sup>3</sup> isosurface.  $\Delta ESP_{\text{meta}} = ESP_{\text{solv}\times 1} - ESP_{\text{gas}}$  as represented by the dotted lines in Figure 2. Error bars represent the error standard deviation of electrostatic potential readings taken over both *meta* positions on each face of the aromatic ring.

Figure 4 show that through-space electrostatic effects are clearly significant, but only partially account for the change in the ESP of the aromatic ring upon substituent solvation ( $\Delta ESP_{\text{meta}}$ ). The difference between  $ESP_{\text{through-space}}$  and  $\Delta ESP_{\text{meta}}$  is due to polarization effects not being taken into account in the through-space model. Nonetheless, the sum of  $ESP_{\text{through-space}} + ESP_{\text{gas}}$  correlated with experimental  $\Delta G$  values better than  $ESP_{\text{gas}}$ , though not quite as well as  $ESP_{\text{solv}\times 1}$  which takes both through-space and polarization effects into account (Table 1 and Figure S13).

In summary, high-quality correlations of experimental conformational free energies with calculated electrostatic potentials indicate that explicit solvation of substituents results in substantial modulation of the electrostatic potentials of aromatic rings. Our success in modeling the solvation of substituents with a single explicit solvent molecule may be attributed to three factors. First, solvents have high molarities (from 10.3 M for CCl<sub>4</sub> to 15.6 M for CD<sub>2</sub>Cl<sub>2</sub>), which means that primary solvation sites will be highly occupied. Second, the primary modes of solvation are easily identified since the substituents and solvents examined here have clearly defined hydrogen-bond donor and acceptor sites. Finally, although the solvation of sites other than the substituents will undoubtedly influence the position of the conformational equilibrium, these effects only appear to influence the gradient of the  $\Delta G$  correlations, but not the scatter seen in these plots. Combined, these favorable circumstances mean that it is possible to attribute the scatter seen the  $\Delta G_{\text{exp}}$  correlations to the electronic effects arising from substituent solvation (which we show can be modeled using modest DFT calculations that include a single explicit solvent molecule). It is important to note that modeling entire systems featuring a Boltzmann distribution of multiple solvated states remains highly challenging, particularly when multiple solvent molecules are

involved (see Table S1). Despite this caveat, we also show that additive through-space electrostatic effects provide a reasonable account of our experimental data, which advocates the use of appropriately parametrized force-field methods for modeling these types of solvent effects with low computational cost. Thus, we hope that these results might contribute to the continued development of explicit,<sup>8</sup> implicit (continuum),<sup>45</sup> and hybrid solvation models.<sup>46</sup>

## ■ ASSOCIATED CONTENT

### ● Supporting Information

Experimental and computational procedures, tables of data, additional correlations, and compound characterization. This material is available free of charge via the Internet at <http://pubs.acs.org>.

## ■ AUTHOR INFORMATION

### Corresponding Author

scott.cockroft@ed.ac.uk

### Notes

The authors declare no competing financial interest.

## ■ ACKNOWLEDGMENTS

We thank EPSRC grant EP/H021620-1, Pfizer Ltd., and the School of Chemistry for funding Ph.D. studentships for K.B.M., C.A., and I.K.M., respectively.

## ■ REFERENCES

- (1) Murray, J. S.; Sen, K. *Molecular Electrostatic Potentials: Concepts and Applications*; Elsevier: Amsterdam, 1996.
- (2) Saggiu, M.; Levinson, N. M.; Boxer, S. G. *J. Am. Chem. Soc.* **2012**, *134*, 18986–18997.
- (3) Hunter, C. A. *Angew. Chem., Int. Ed.* **2004**, *43*, 5310–5324.
- (4) Zheng, J.; Kwak, K.; Asbury, J.; Chen, X.; Piletic, I. R.; Fayer, M. D. *Science* **2005**, *309*, 1338–1343.
- (5) Reichard, C. *Solvents and Solvent Effects in Organic Chemistry*, 3rd ed.; Wiley-VCH: Weinheim, 2003.
- (6) Otto, R.; Brox, J.; Trippel, S.; Stei, M.; Best, T.; Wester, R. *Nat. Chem.* **2012**, *4*, 534–538.
- (7) Gronert, S.; Pratt, L. M.; Mogali, S. *J. Am. Chem. Soc.* **2001**, *123*, 3081–3091.
- (8) Genheden, S.; Mikulskis, P.; Hu, L.; Kongsted, J.; Söderhjelm, P.; Ryde, U. *J. Am. Chem. Soc.* **2011**, *133*, 13081–13092.
- (9) Mati, I. K.; Cockroft, S. L. *Chem. Soc. Rev.* **2010**, *39*, 4195–4205.
- (10) Hof, F.; Scofield, D. M.; Schweizer, W. B.; Diederich, F. *Angew. Chem., Int. Ed.* **2004**, *43*, 5056–5059.
- (11) Cockroft, S. L.; Hunter, C. A. *Chem. Commun.* **2009**, 3961–3963.
- (12) Gung, B. W.; Patel, M.; Xue, X. *J. Org. Chem.* **2005**, *70*, 10532–10537.
- (13) Cozzi, F.; Cinquini, M.; Annuziata, R.; Siegel, J. S. *J. Am. Chem. Soc.* **1993**, *115*, 5330–5331.
- (14) Fischer, F. R.; Wood, P. A.; Allen, F. H.; Diederich, F. *Proc. Natl. Acad. Sci. U.S.A.* **2008**, *105*, 17290–17294.
- (15) Gardner, R. R.; McKay, S. L.; Gellman, S. H. *Org. Lett.* **2000**, *2*, 2335–2338.
- (16) Chapman, K. T.; Still, W. C. *J. Am. Chem. Soc.* **1989**, *111*, 3075–3077.
- (17) Ferguson, S. B.; Sanford, E. M.; Seward, E. M.; Diederich, F. *J. Am. Chem. Soc.* **1991**, *113*, 5410–5419.
- (18) Ando, S.; Ohta, E.; Kosaka, A.; Hashizume, D.; Koshino, H.; Fukushima, T.; Aida, T. *J. Am. Chem. Soc.* **2012**, *134*, 11084–11087.
- (19) Bhayana, B.; Wilcox, C. S. *Angew. Chem., Int. Ed.* **2007**, *46*, 6833–6836.
- (20) Fujio, M.; McIver, R. T.; Taft, R. W. *J. Am. Chem. Soc.* **1981**, *103*, 4017–4029.
- (21) Headley, A. D. *J. Chem. Soc., Perkin Trans. 2* **1989**, 457–461.
- (22) Mashima, M.; McIver, R.; Taft, R. *J. Am. Chem. Soc.* **1984**, *106*, 2717–2718.
- (23) Ōki, M. *Acc. Chem. Res.* **1990**, *23*, 351–356.
- (24) Paliwal, S.; Geib, S.; Wilcox, C. S. *J. Am. Chem. Soc.* **1994**, *116*, 4497–4498.
- (25) Kim, E.-i.; Paliwal, S.; Wilcox, C. S. *J. Am. Chem. Soc.* **1998**, *120*, 11192–11193.
- (26) Carroll, W. R.; Pellechia, P.; Shimizu, K. D. *Org. Lett.* **2008**, *10*, 3547–3550.
- (27) Zhao, C.; Parrish, R. M.; Smith, M. D.; Pellechia, P. J.; Sherrill, C. D.; Shimizu, K. D. *J. Am. Chem. Soc.* **2012**, *134*, 14306–14309.
- (28) Gung, B. W.; Emenike, B. U.; Lewis, M.; Kirschbaum, K. *Chem.—Eur. J.* **2010**, *16*, 12357–12362.
- (29) Motherwell, W. B.; Moise, J.; Aliev, A. E.; Nic, M.; Coles, S. J.; Horton, P. N.; Hursthouse, M. B.; Chessari, G.; Hunter, C. A.; Vinter, J. G. *Angew. Chem., Int. Ed.* **2007**, *46*, 7823–7826.
- (30) Cozzi, F.; Siegel, J. S. *Pure Appl. Chem.* **1995**, *67*, 683–9.
- (31) Newcomb, L. F.; Gellman, S. H. *J. Am. Chem. Soc.* **1994**, *116*, 4993–4994.
- (32) Nakamura, K.; Houk, K. N. *Org. Lett.* **1999**, *1*, 2049–2051.
- (33) Fischer, F. R.; Schweizer, W. B.; Diederich, F. *Angew. Chem., Int. Ed.* **2007**, *46*, 8270–8273.
- (34) Hammett substituent constants have been used to rationalize an enormous range of processes occurring in organic solution despite  $\sigma_m$  and  $\sigma_p$  being measured in water. This is classically attributed to the transferability of the intramolecular electronic effects of substituents. Indeed, this is also the case in our system, where the electronic effects of substituents dominate across all solvents, while substituent solvation manifests itself as scattering in the  $\Delta G$  correlations.
- (35) Randell, K. D.; Johnston, B. D.; Green, D. F.; Pinto, B. M. *J. Org. Chem.* **1999**, *65*, 220–226.
- (36) Hunter, C. A.; Low, C. M. R.; Vinter, J. G.; Zonta, C. *J. Am. Chem. Soc.* **2003**, *125*, 9936–9937.
- (37) Cockroft, S. L.; Hunter, C. A. *Chem. Soc. Rev.* **2007**, *36*, 172–188.
- (38) Carver, F. J.; Hunter, C. A.; Livingstone, D. J.; McCabe, J. F.; Seward, E. M. *Chem.—Eur. J.* **2002**, *8*, 2847–2859.
- (39) Cockroft, S. L.; Hunter, C. A.; Lawson, K. R.; Perkins, J.; Urch, C. J. *J. Am. Chem. Soc.* **2005**, *127*, 8594–8595.
- (40) Cockroft, S. L.; Perkins, J.; Zonta, C.; Adams, H.; Spey, S. E.; Low, C. M. R.; Vinter, J. G.; Lawson, K. R.; Urch, C. J.; Hunter, C. A. *Org. Biomol. Chem.* **2007**, *5*, 1062–1080.
- (41) Wheeler, S. E. *J. Am. Chem. Soc.* **2011**, *133*, 10262–10274.
- (42) Wheeler, S. E.; Houk, K. N. *J. Chem. Theory Comput.* **2009**, *5*, 2301–2312.
- (43) Bisson, A. P.; Hunter, C. A.; Morales, J. C.; Young, K. *Chem.—Eur. J.* **1998**, *4*, 845–851.
- (44) Sayyed, F. B.; Suresh, C. H.; Gadre, S. R. *J. Phys. Chem. A* **2010**, *114*, 12330–12333.
- (45) Cramer, C. J.; Truhlar, D. G. *Chem. Rev.* **1999**, *99*, 2161–2200.
- (46) da Silva, E. F.; Svendsen, H. F.; Merz, K. M. *J. Phys. Chem. A* **2009**, *113*, 6404–6409.